Kasai *et al.*
Progress in Earth and Planetary Science (2024) 11:21
https://doi.org/10.1186/s40645-024-00626-x

Progress in Earth and Planetary Science

RESEARCH ARTICLE

Open Access

Quantification of the spatial distribution of individual mangrove tree species derived from LiDAR point clouds

Katsumi Kasai[1*], Hideaki Yanagisawa[2] and Kazuhisa Goto[1]

Abstract

Mangrove forests have unquestionably high environmental and ecological value. Mangrove trees are believed to have habitat zonation that is controlled mainly by the relative sea level. However, earlier discussions of mangrove habitats have remained limited in terms of their quality and quantity because of a lack of high-resolution spatial information of microtopography and trees. To clarify mangrove habitability over a wide forest area, we compounded mobile laser scanning (MLS) and aerial laser scanning (ALS) LiDAR dataset of the Miyara River mangrove on Ishigaki Island, Okinawa, Japan. The MLS provided sub-canopy data, while the unmanned aerial vehicle ALS data mainly provided a point cloud of the canopy. We corrected point clouds and combined these data. The results indicated that ALS is unable to reconstruct the microtopography of the dense mangrove area well. Moreover, tree species were not identifiable from the ALS data. However, by applying MLS to the mangrove forest, we obtained high-resolution microtopography and tree information inside the forest, although the measurement area was limited to comparison with ALS. By combining ALS and MLS point clouds, 3D point clouds of the forest were well reconstructed. From these point clouds, a high-resolution digital elevation model was created. Subsequently, we segmented trees individually from composite MLS point clouds and identified each tree species. Consequently, the spatial distribution of thousands of mangrove trees was reconstructed at the Miyara River mouth. The spatial distribution of mangrove tree species together with earlier aerial photographs suggests that mangrove species have been segregated in accordance with changes in their elevation and environment over 40 years. Our findings suggest that the distribution of the species changed sensitively along with dynamic variation of the microtopography.

Keywords LiDAR, UAV, SLAM, *Bruguiera gymnorrhiza*, Ishigaki Island, Mangrove, *Rhizophora stylosa*, Zonation, Miyara River

1 Introduction

Mangroves characteristically inhabit areas above mean sea level (MSL) in intertidal zones of tropical and subtropical coasts (Macnae 1969; Woodroffe et al. 2016). For recently examined mangrove habitats, vertical accreting thick sequences of organic sediments occur primarily due to a rate of relative sea-level rise (Saintilan et al. 2020). Mangrove habitats typically show a zonation pattern: dominant species are mainly replaced depending on elevation change (Duke et al. 1998; Mochida et al. 1999). Consequently, mangrove tree species inhabit limited elevation ranges, which shifts over time in accordance with the relative sea-level changes. Such relative sea-level changes might happen not only by absolute sea level changes but also by the microtopographic changes such as uplift and subsidence of ground elevation by seismic

*Correspondence:
Katsumi Kasai
kasai-katsumi0316@g.ecc.u-tokyo.ac.jp
[1] Department of Earth and Planetary Science, The University of Tokyo, 7-3-1 Hongo, Bunkyo-ku, Tokyo 113-0033, Japan
[2] Department of Regional Communication Studies, Faculty of Regional Studies, Tohoku Gakuin University, 3-1 Shimizukoji, Wakabayashi-ku, Sendai, Miyagi 980-8511, Japan

activities and by the deposition and erosion of the sediments in association with floods and other phenomena. To elucidate the mangrove habitat dynamics, some studies have tracked the horizontal distribution areas of mangrove forest by comparison with earlier aerial photographs (Do et al. 2022). Nevertheless, these studies are few because it is difficult to map individual tree species using remote sensing techniques (Pham et al. 2019). Moreover, understanding the microtopography within mangrove forests is difficult because some mangrove species have overhanging prop roots; also, the forests often have dense accumulations of trees and are submerged by tides every day (Yang et al. 2022; You et al. 2023). These environments make it difficult to conventional surveying in mangrove forests, and it is difficult to conduct topographic surveys efficiently and precisely in a short time. Therefore, a small number of people and a short period of surveying cannot easily understand the microtopography and forest conditions over a wide area. Although there are some pioneering efforts to investigate the relationship between microtopography and tree species distribution (e.g., Fujimoto et al. 1995), such works are very limited nevertheless of the importance in mangrove science. This is probably because measurement of microtopography and tree species is time-consuming and development of efficient methods has long been awaited. Indeed, earlier field investigations have been mostly qualitative or, even when quantitative, based on limited information of a narrow area. Therefore, the actual relation between mangrove habitats and microtopography has not been sufficiently elucidated yet. Obtaining sufficient quality and quantity of microtopography and tree data is the barrier which must be hurdled for investigations of mangrove habitability.

To overcome these limitations of earlier studies, light detection and ranging (LiDAR) is the breakthrough survey technique. LiDAR technique can be divided into three survey techniques: (1) aerial laser scanning (ALS), which measures the ground from the sky using a small aircraft or UAV; (2) mobile laser scanning (MLS), which obtains measurements while a researcher walks using handheld equipment; and (3) terrestrial laser scanning (TLS), which measures target objects from a fixed location (Donager et al. 2021). Yin and Wang (2019) recommended a combination of ALS and TLS to improve surveys of mangrove forests. Unfortunately, TLS is unsuitable for topographic and tree surveys of the mangrove forest over a wide area because of its requirement for many scans at different points. In general, TLS-based field measurements take approximately ten hours for a plot of 100 m × 100 m (Shao et al. 2020). Although ALS is a promising technique to measure mangrove forests and although it has been used for recent studies (Yin and Wang 2019; You et al. 2023), its laser might not reach the ground surface. In such cases, the quality of the obtained topographic data would depend on tree canopy shading. In addition, ALS might be unable to produce point clouds of tree shapes because the tree canopy would shade tree trunks and roots. Knight et al. (2009) stated that ALS is effective in forests with low to medium canopy density, but the ALS performance might be limited at dense mangrove forests. Tong et al. (2023) reported that the root mean-squared error (RMSE) of DEM obtained using UAV aerial photographs relative to ground control points (GCP) in the mangrove forest is 0.281 m. This accuracy makes it difficult not only to discuss the habitat elevation range of each mangrove species in a narrow intertidal zone, but also the microtopography in mangrove forests. Therefore, using ALS alone for ecological studies such as elucidating the spatial distribution of tree species is difficult. However, few studies have conducted MLS surveys of mangrove forests (Niwa et al. 2023; Yamamoto et al. 2023). In Niwa et al. (2023); they applied two types of LiDAR survey (ALS and MLS) in the mangrove forest. They stated that combining point clouds from ALS and MLS platforms in mangrove forest topographic surveys can yield better accurate data. However, errors specific to each platform have not been considered, and there is a need for accuracy verification. Also, relationship between microtopography and mangrove tree distributions have not been explored in this research. The need exists to verify accuracy and to evaluate an appropriate processing scheme. If the point clouds obtained by ALS and MLS can be combined accurately, then they might be able to complement each other's blind spots and provide a representation (Nakata et al. 2023) with highly accurate 3D data of mangrove forests, including relationship between topography and distribution of tree species. Despite that promise, no report of the literature has described an attempt to do so.

If the topography in mangrove forests can be reconstructed over a wide area with higher accuracy, and if the spatial distribution of trees can be measured, these data will constitute a promising fundamental dataset for future geomorphological and ecological studies in the mangrove forest. The objective of this study is to ascertain the spatial distribution of individual mangrove tree species quantitatively over a wide area and to identify the factors affecting their habitability, especially in relation to microtopography in mangrove forests. For this objective, we obtained highly accurate microtopographic data in mangrove forests over a wide area by combining LiDAR surveys of two types (ALS + MLS). The obtained point clouds were corrected, combined, verified for their accuracy, and then created using high-resolution DEM. The spatial distribution of each mangrove tree species was

also obtained by segmenting individual trees and visually sorting from LiDAR data and DEM. Finally, vegetation changes taking place over 40 years in the mangrove forest were discussed based on a comparison of past aerial photograph and newly obtained spatial distributions of mangrove tree species.

2 Methods

2.1 Site setting

This research was conducted in the Miyara River mouth, Ishigaki Island, Okinawa, Japan (Fig. 1). This forest was selected because it is a compact area for ALS and because it is walkable with MLS, although its canopy shading rate is high. The Miyara River, which drains the southeastern part of Ishigaki Island, is about 12 km long, has an approximately 36 km^2 basin area. The mangrove forest covers 0.15 km^2 of estuary, with mangrove tree species predominantly of *Bruguiera gymnorrhiza*, *Rhizophora stylosa*, and *Kandelia obovata* (Yamada et al. 2013).

2.2 LiDAR survey

We performed LiDAR surveys of two types: ALS from the sky using a real-time kinematic (RTK)-UAV, and MLS within the forest using backpack-mounted LiDAR with simultaneous localization and mapping (SLAM) technology. Because laser light cannot capture the underwater topography, surveys were conducted at the time of spring low tide to capture intertidal topography as possible. The output coordinate system used for the data was Japan Geodetic System 2011 (EPSG: 6684). The elevation datum applied to the data is the Tokyo Peil (T.P.). The MSL at the Ishigaki Port during 2017–2021, which was the closest observation point to the study site and measured by Japan Meteorological Agency (JMA), is 15.9 cm above T.P.

2.2.1 ALS

The point clouds of the ALS were acquired using the DJI UAV LiDAR platform, specifically Matrice 300 RTK (DJI, China) was used with the LiDAR equipment (Zenmuse L1; DJI, China). It has a 20-megapixel camera, inertial motion unit (IMU), and laser sensor installed in it. Therefore, point clouds and aerial photographs can be acquired simultaneously during the same flight. The viewing angle is 70.4°. The measurement range is within 190 m when reflectivity is > 10%. The laser generates 160,000 per second. From 50 m altitude, the measurement error is within 10 cm in the horizontal direction and within 5 cm in the vertical direction. Point clouds were collected by RTK positioning. A mobile station (D-RTK 2; DJI Inc., China) was used as the base station. The coordinate of the base station was determined by static positioning with a GNSS receiver (Trimble R2; Trimble Navigation Ltd., USA). Then, coordinates and elevations were assigned to the acquired point clouds and aerial photographs.

When flying at 50 m altitude from the base station on July 14, 2022, the ALS data were acquired. Software (DJI Terra; DJI, China) was used for data post-processing. By providing the coordinate and elevation of the base station, point cloud data were acquired with them.

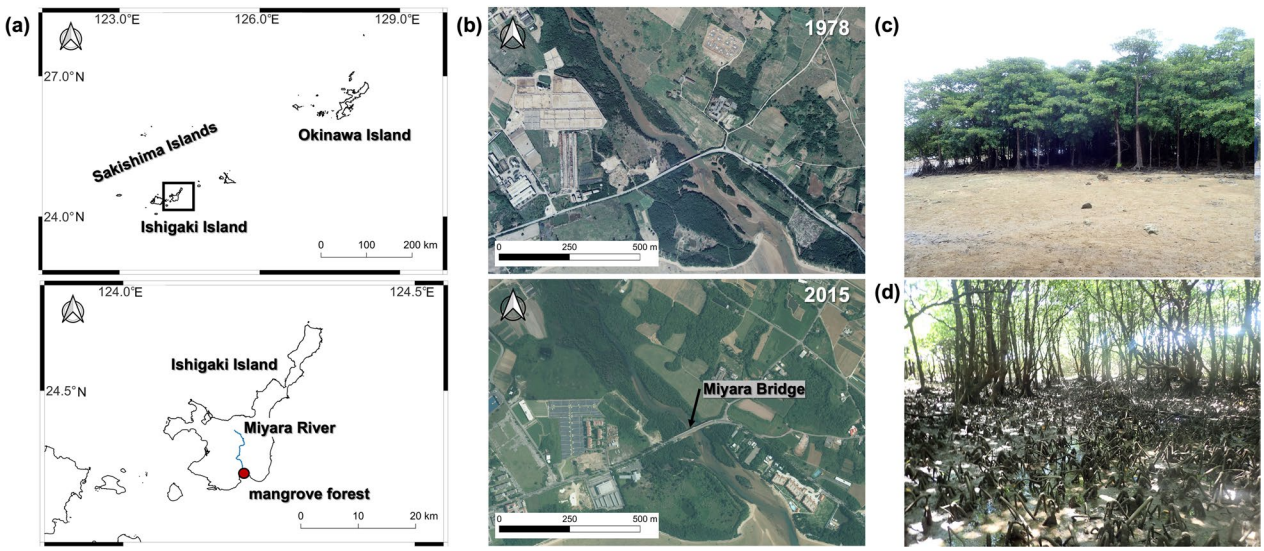

Fig. 1 **a** Map showing the Miyara River mangrove forest location on Ishigaki Island of the Sakishima Islands, Okinawa, Japan. **b** Aerial photographs of the study area in 1978 and 2015. The aerial photographs were provided by the Geospatial Information Authority of Japan. **c** View of the Miyara River mangrove forest downstream from the Miyara Bridge. The tree species are being replaced from the river (left hand) to the inland area (right hand). **d** Small creek in the mangrove forest. It is not visible in aerial photographs because of canopy shading

Orthophoto was created using Metashape (Agisoft LLC, Russia) from aerial photographs acquired during the ALS survey. After two flights (total about 45 min), ALS point clouds from the UAV had been acquired and an area of about 22 ha was surveyed.

2.2.2 MLS

A backpack-style LiDAR with a SLAM system was used for MLS. SLAM can estimate its own position by matching characteristic points and allowing us to obtain accurate positions even in a forest that hampers the GNSS signal (Hyyppä et al. 2020). The matching of characteristic points is based on photographs correspondence. LiBackpack GC50 (GreenValley International, USA) was used for the MLS survey. This equipment has a laser sensor, a GNSS receiver, and a 360° camera. The viewing angle is vertical of ± 15° and fully 360° horizontally. The measurement range is within 100 m at the place where reflectivity is > 20%. The laser beam is 300,000 shots per second. Measurement error is within 3 cm. A 360° camera was used to take movie files simultaneously with acquisition of the point cloud. Data acquisition was conducted on November 5 and 6, 2022, by a person carrying MLS and walking in a loop through the mangrove forest to avoid crossing the route. The routes were selected after looking at ALS-DEM to cover the areas in which no ALS-DEM data were obtained because of the high canopy shielding rate. A GNSS base station was placed in a location with open sky for differential positioning by post-processing. The starting and ending places of the walking route were selected at locations with open sky where stable GNSS signals were able to be acquired. It is known that SLAM accumulates cumulative error over measurement time (Xie et al. 2022). For this reason, to reduce the time of each run, measurements were taken seven times using different routes (four times on November 5, 2022; three times on November 6, 2022). The measurement time of each run was about 10 min.

For data processing, the software LiFuser BP (Green Valley International, USA) was used. After the acquired point cloud data were imported into the software, the characteristic points were matched before and after the frame. Then, by providing the location and elevation of the base station, point cloud data were acquired with coordinate and elevation. In addition, color information was added from 360° camera images. Position correction was performed using GNSS information from the reference station. Then SLAM reanalysis was performed. Also point clouds that were judged as unreliable, such as points captured below the water surface where the laser could not possibly reach, or scattered points at the edge of the point cloud, were removed manually.

2.2.3 Evaluation of precision

GNSS surveys were conducted in November 2022 and June 2023 to measure the coordinates of reference points for accuracy verification of ALS and MLS. Drogger (BizStation Corp., Japan) and Promark120 (Trimble Inc., USA) were used for surveying. Post-processing corrections were applied at the GNSS-based Control Station of the Geospatial Information Authority of Japan. The accuracy of Drogger is typically within a few centimeters under environments in which they are recommended for use (Ishikawa et al. 2022). We measured 12 points (Table 1). However, the area is covered mainly by the forest and artificial objects so that coordinates of some points were unsuitable for the evaluation because of canopy shielding or artificial metal objects. To evaluate their accuracies, we plotted the data on a GIS and compared GNSS points with aerial photographs. Then, we excluded survey points whose locations were clearly different (Table 1). Reference points P1, P3, P5, P9, and P12 were excluded from ALS point accuracy evaluation because they were clearly out of alignment with the measurement place when they were plotted on the GIS. In addition, points P7 indicating z values that differ from DEM (z value of point P7 is on the bridge, but z value of DEM is on the ground under the bridge) and P2 falling outside DEM area were excluded from the DEM accuracy evaluation. We used seven points as reference for ALS and five points as accuracy verification for DEM.

2.3 Data analysis

For point cloud analyses, LiDAR360 (GreenValley International, USA) and Cloud Compare were used. With LiDAR360, we corrected and combined point clouds, classified ground points using high-density TIN filtering based on Zhao et al. (2016), created a 0.5 m mesh DEM, and did tree species segmentation. However, we realized that LiDAR360 alone was insufficient to classify ground points well. Therefore, to create a better quality of DEM, we first classified ground points using the cloth simulation filter (CSF) based on Zhang et al. (2016) provided with Cloud Compare. Then, we classified the ground points again using LiDAR360. Point clouds were also corrected in Cloud Compare.

2.3.1 Alignment and combination of point clouds

The seven MLS point clouds were combined as explained hereinafter. First, two MLS point clouds upstream of the Miyara Bridge and five MLS point clouds downstream of the Miyara Bridge were combined. The MLS point clouds, in which cumulative errors had accumulated, were extracted by several time ranges. Then each was combined. When combining MLS point clouds, we manually

Table 1 Accuracy evaluation of ALS point clouds and DEM by reference points

	Reference point			ALS			DEM	ALS error (m)		DEM error (m)	Remarks
	x	*y*	*z*	*x*	*y*	*z*	*z*	Horizontal	Vertical		
P1	21,417.7973	− 181,823.644	2.406	21,415.905	− 181,824.063	2.494	0.64416	–	–	–	Alongside the bridge structure
P2	21,397.5107	− 181,826.9974	5.275	21,397.599	− 181,826.956	5.369	–	0.097523587	0.094	–	Point outside the DEM
P3	21,427.9364	− 181,819.1984	0.831	21,429.953	− 181,819.101	0.889	0.81702	–	–	–	Alongside the tree canopy
P4	21,367.2226	− 181,925.6136	0.326	21,366.405	− 181,925.666	0.428	0.39588	0.819277438	0.102	0.06988	
P5	21,468.486	− 181,796.9861	7.271	21,463.728	− 181,796.13	7.496	− 0.3383	–	–	–	On the bridge
P6	21,366.45	− 181,922.091	0.2929	21,366.472	− 181,922.054	0.368	0.346	0.043046486	0.0751	0.0531	
P7	21,463.275	− 181,796.294	7.31	21,463.259	− 181,796.339	7.46	− 0.1786	0.047759816	0.15	–	On the bridge
P8	21,369.714	− 181,737.606	0.1061	21,369.675	− 181,737.646	0.101	− 0.2133	0.055865911	0.0051	0.31938	
P9	21,406.48	− 181,805.46	1.9769	21,407.503	− 181,805.776	2.448	− 0.1335	–	–	–	Alongside the bridge structure
P10	21,431.488	− 181,818.516	0.8242	21,431.54	− 181,818.517	0.881	0.81866	0.052009614	0.0568	0.00554	
P11	21,480.24	− 181,833.655	− 0.0487	21,480.334	− 181,833.577	− 0.04	− 0.0311	0.122147452	0.0087	0.01756	
P12	21,404.474	− 181,782.139	0.2773	21,405.116	− 181,782.225	0.223	0.15956	–	–	–	Under the tree canopy
										DEM MAE (m)	0.093092
										DEM RMSE (m)	0.148354612

selected up to four points, where are expected to represent the same points between alignment point clouds of one MLS and reference point clouds of the other MLS, and transformed alignment point clouds using a matrix. This matrix applied to alignment point clouds minimized location errors resulting from the differences of these point clouds when combined. Alternatively, manual rotation and translation were used in combination, if required. The GNSS information of the point clouds was not obtained for the three MLS point clouds on November 6 because the base station had not functioned properly. These data were therefore combined with the point cloud for the four surveys on November 5, which have GNSS information by matrix transformation. The total area of the composite MLS point clouds was about 2.5 ha. Then, composite MLS point clouds that were made from all seven MLS point clouds were corrected further by the ALS point clouds, the latter of which cover a wider area. Manual rotation and translation were used as alignment. Finally, composite ALS + MLS point clouds were created.

2.3.2 Tree species segmentation

The Point Cloud Segmentation function of LiDAR360 was used for mangrove tree segmentation. Point Cloud Segmentation function was developed originally as an algorithm to segment individual trees from TLS point clouds (Li et al. 2012) but it is also applicable to MLS point clouds. An earlier study using backpack LiDAR in forest to segment trees with this function reported an 88% detection rate with 83% segmentation accuracy (Liu et al. 2023). According to Niwa et al. (2023), it is stated that the number of recognized trees in the segmentation results of mangrove forest MLS point clouds, using the default parameter of this function, was approximately twice that of visually identified results. We identified all tree species manually by shape from composite MLS point clouds segmented using the Point Cloud Segmentation function. Although most trees were individually recognized well, multiple trees were detected as one tree in some cases. To address that problem, we manually checked and split them to assign each coordinate and species. Moreover, we used the 360° camera to remove objects that were misidentified as trees or which were non-mangrove tree species. For the segmented and identified trees, elevation values were obtained from the DEM data. The habitat altitude ranges were calculated for each tree species.

2.3.3 Comparison with past aerial photographs

Although the LiDAR survey can provide detailed information about the current mangrove distribution and the microtopography in mangrove forests, it cannot assess the history because there are no past point cloud data of mangrove forests in the Miyara River. However, to discuss the factors controlling mangrove habitats, it is important to understand the process by which the current mangrove forests have changed. Therefore, for this study, by using past aerial photographs from the Geospatial Information Authority of Japan, the present distribution of mangrove forest was compared with the earlier state of the mangrove forest.

By comparison of past aerial photographs, Nakaza et al. (2011) pointed out that the distribution area of Miyara River mangrove forest was increased and that some part of the river was partially blocked during 1967–2006. For this study, earlier aerial color photographs taken in 1978, which the mangrove forest locates in the center and no clouds were reflected in the image, were used for comparison. The earlier aerial photograph was rasterized using ArcGIS Pro (ESRI Inc., USA), and was overlaid with the orthophoto that was created from aerial photographs by UAV. The Visible Atmospherically Resistant Index (VARI) values defined by Gitelson et al. (2002) were used for comparison. Through the heuristic investigation, the locations where the value increased by more than 0.15 were defined in this study as locations where vegetation had increased.

3 Results

3.1 Results of LiDAR surveys and data combination

Comparison of the coordinates between the point clouds obtained by the ALS (Fig. 2) and reference points showed that the error was within 0.81 m (0.12 m, with one exceptional value) in horizontal direction and within 0.15 m in vertical direction (Table 1). These values are similar with the accuracy of the device itself. Therefore, the ALS point clouds can be used as a reference to correct composite MLS point clouds (Fig. 3a, b). Then, comparison of the elevations between the DEM created from composite ALS + MLS point clouds and reference points showed that the mean absolute error (MAE) was 0.0931 m and that the RMSE was 0.148 m. These values have sufficiently high accuracy compared to those produced by earlier studies (Tong et al. 2023).

3.2 Reconstruction of microtopography in the mangrove forest

At the study site, there was a "no data" area in the DEM created solely from the ALS point clouds (Fig. 4). To create DEM, sufficient ground points must be obtained. However, depending on the shielding ratio by tree canopies at the Miyara River mangrove forest, the laser was sometimes unable to reach to the ground surface. For that reason, sufficient ground points were not obtained using ALS. It is noteworthy that shapes associated with each tree such as trunks and branches could not be

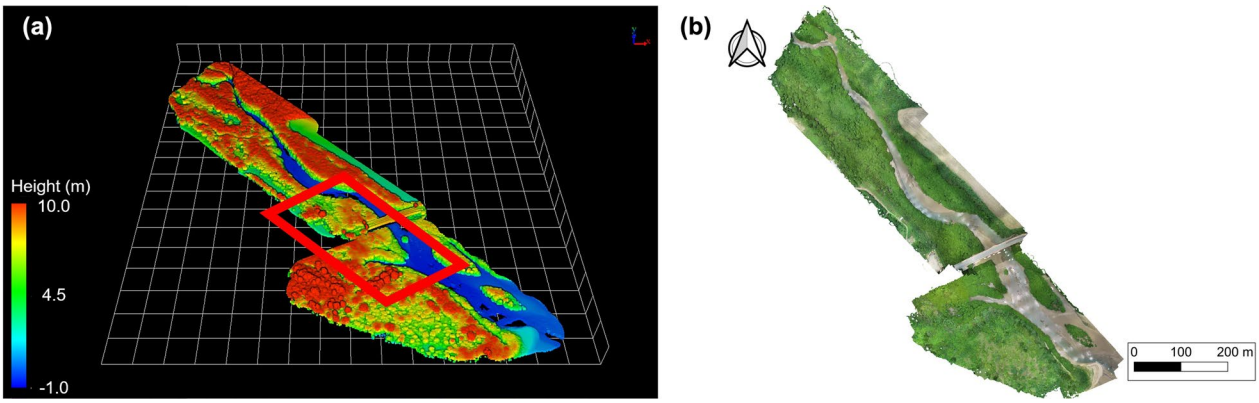

Fig. 2 **a** ALS point clouds. Background grids are 50 m. An area of about 22 ha was surveyed. The red square marks the area surveyed by MLS in Fig. 3. **b** Orthophoto created from aerial photographs obtained from an ALS survey

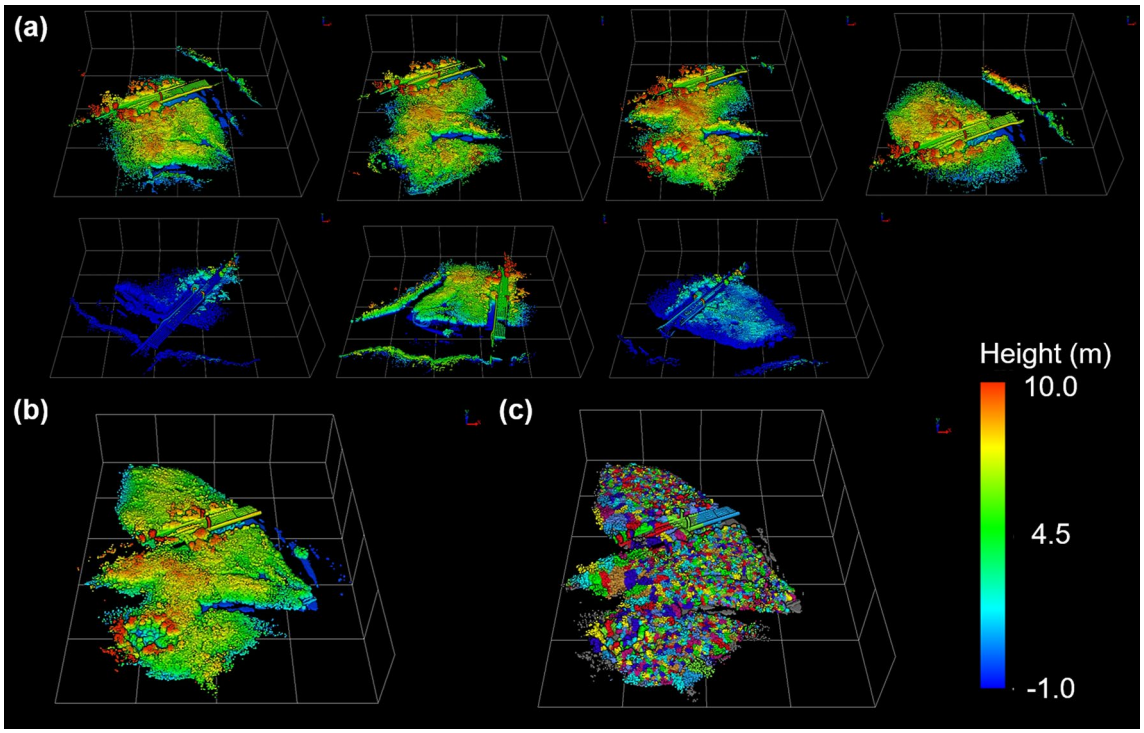

Fig. 3 Results of MLS surveys. Background grids are 50 m. **a** Seven point clouds obtained from each MLS survey. The three point clouds in the lower panel did not have GNSS information at raw data. Therefore, they show different elevations and directions. **b** A composite MLS point clouds for the location in Fig. 2a. The total area was about 2.5 ha. **c** Result of tree segmentation from composite MLS point clouds

detected from the ALS point clouds, simply because ALS measures the trees perpendicularly from the sky.

This shortcoming of ALS can be complemented by MLS point clouds. This complementarity can be achieved because MLS can measure inside of the forest so that not only the ground surface but also tree shapes are measurable, although tree canopies, which can be obtainable by ALS, are not measurable by MLS. As a result of the combination with ALS and MLS point clouds, ground points, where there were "no data" in the ALS-DEM, were well complemented by composite MLS point clouds (Fig. 5).

The final DEM, which combined ALS + MLS point clouds and which is 0.5 m mesh, shows that elevation of mangrove forest is approx. − 0.73 to 1.17 m. In this DEM, microtopographical features such as small creeks

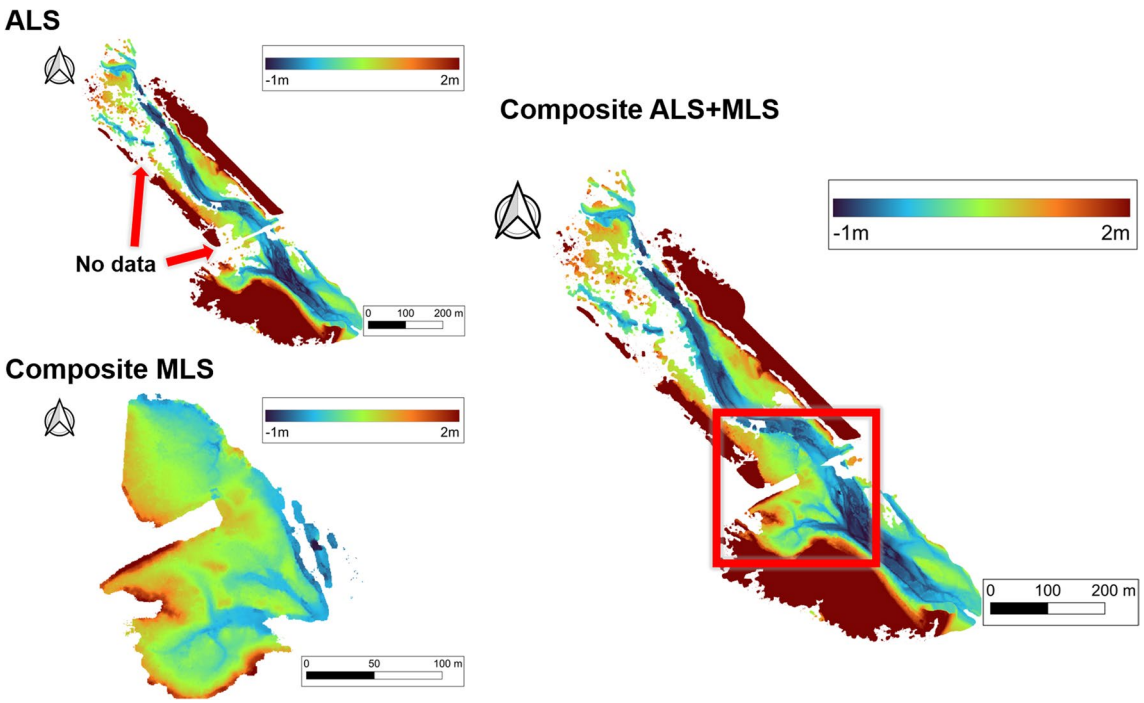

Fig. 4 DEM created from ALS point clouds (left top), composite MLS point clouds (left bottom), and composite ALS + MLS point clouds (right). By combining ALS and MLS point clouds, the area (red square) in which there were "no data" in the ALS-DEM was well complemented by composite MLS point clouds

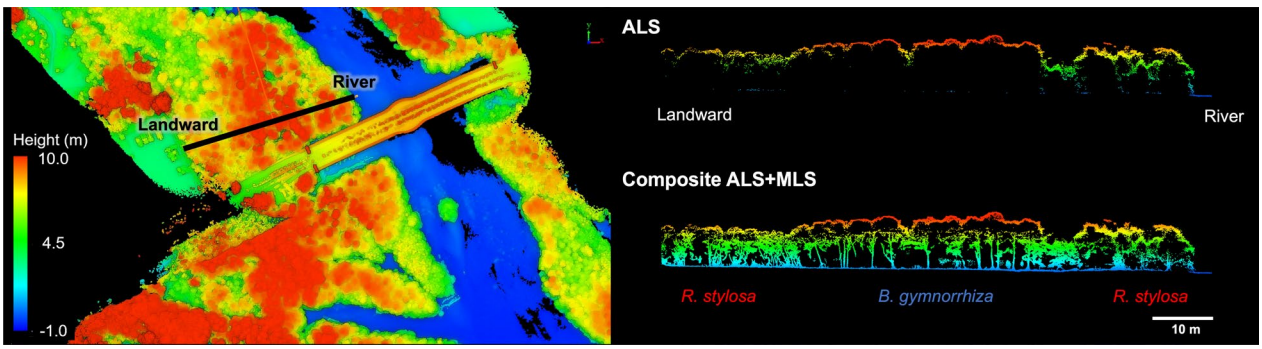

Fig. 5 Profile view in the mangrove forest. Transect position (left). Transect profiles of ALS point clouds (right top) and composite ALS + MLS point clouds (right bottom). The combination of ALS and composite MLS point clouds shows the complementation of ground points and tree shapes. Moreover, it is apparent that the elevation increases gradually from the river to land. Changes in tree species are visible

are recognizable throughout the mangrove forest. These microtopographies are not observable from aerial photographs because they were hidden by dense tree canopies. It also shows that the elevation increases away from the river and creeks. The elevation increases rapidly to over 2 m at the inland edge of the forest.

3.3 Mangrove distribution

As a result of tree species segmentation (Fig. 3c), 4106 trees were detected in total: those are 2553 trees of *Bruguiera gymnorrhiza*, 1474 trees of *Rhizophora stylosa*, and 79 trees for which the tree species were judged as saplings with undetermined species or were non-mangrove species (Fig. 6). *Kandelia obovata* was not found by field observations in the MLS survey area. The spatial distribution of tree species shows that *Bruguiera gymnorrhiza* is the dominant species and that it is widely distributed throughout the area. By contrast, *Rhizophora stylosa* is located around the river fronts and creek sides, and around the boundaries between mangroves and

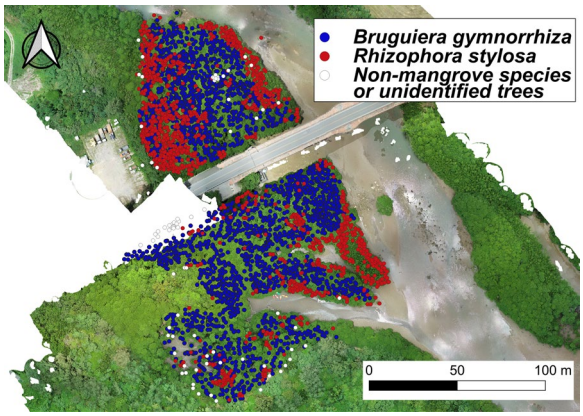

Fig. 6 Distribution of tree species on the orthophoto. *Rhizophora stylosa* (red) is distributed landward, at the riverside, and along creeks to rim *Bruguiera gymnorrhiza* (blue). White circle indicates other trees (non-mangrove trees and unidentified trees)

non-mangrove trees. *Rhizophora stylosa* are also distributed as a rim surrounding the *Bruguiera gymnorrhiza* area.

Because we have high-resolution DEM, the frequency distribution of habitat altitude can be calculated for each tree species (Fig. 7). *Bruguiera gymnorrhiza* inhabits − 0.47 to 1.12 m. *Rhizophora stylosa* inhabits − 0.73 to 1.17 m. In this way, *Rhizophora stylosa* in the Miyara River mangrove forest inhabits a slightly broader range of lower and higher elevations than *Bruguiera gymnorrhiza* does. In addition, *Bruguiera gymnorrhiza* shows a nearly normal distribution with a sharp peak at around 0.4 m. By contrast, *Rhizophora stylosa* has multiple peaks. In addition, *Rhizophora stylosa* individuals are distributed preferentially at lower and higher elevations, where few *Bruguiera gymnorrhiza* individuals live, but they are fewer at around 0.4 m elevation where *Bruguiera gymnorrhiza* individuals are predominant. In this survey area, about 89% of *Bruguiera gymnorrhiza* trees and about 78% of *Rhizophora stylosa* trees were above MSL.

3.4 Comparison with the past aerial photograph

By comparing VARI values of aerial photographs of 1978 and 2022, Fig. 8 shows the areas where the vegetations are thought to have grown during this period. Indeed, as the figure shows, the vegetation area has clearly advanced toward the riverside. It is also noteworthy that the vegetation area has advanced landward in inland areas away from the river. Based on field observations, vegetation at these two expanded area can be characterized as *Rhizophora stylosa*.

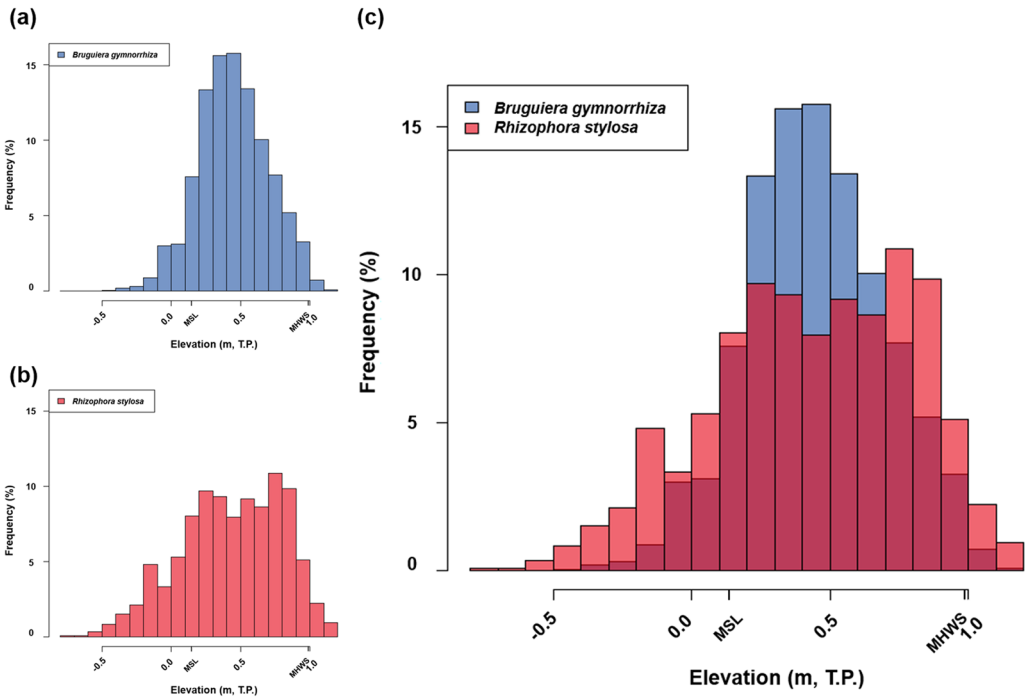

Fig. 7 Frequency distribution of habitat altitude for each mangrove tree species. **a** *Bruguiera gymnorrhiza*, **b** *Rhizophora stylosa*, **c** *Bruguiera gymnorrhiza* and *Rhizophora stylosa*

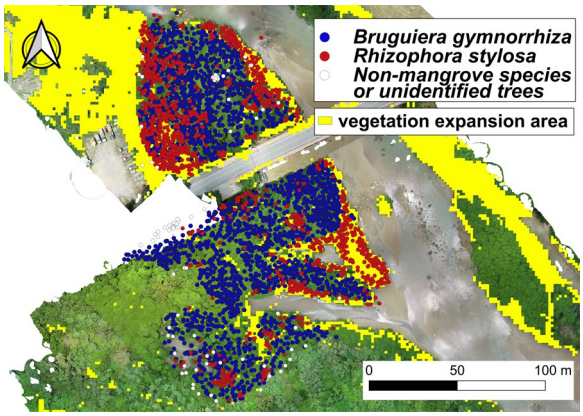

Fig. 8 Map showing locations where the vegetation is regarded as expanding over the last 40 years from the change of VARI values (yellow). Mangrove tree species distributions are also overlapped. The vegetation is shown as expanding at both the riverside and landward. *Rhizophora stylosa* is mainly distributed in vegetation expanded area

4 Discussion

4.1 Distribution characteristics of mangrove trees

The tree species segmentation in this study was conducted within the area which could be surveyed by MLS, whereas areas close to the river were not measured well because the area was not walkable. It is also likely that tree species are not counted accurately in areas where the point cloud density is low. These remaining issues notwithstanding, this study was able to use composite MLS point clouds to elucidate the spatial distribution of mangrove tree species quantitatively over a wide area for the first time ever reported. This achievement marks important progress in the study of tree distributions in mangrove forests: without such high-resolution point clouds, earlier studies could have done similar assessments based solely on field observations, transect survey results (e.g., Mochida et al. 1999; Fujimoto and Ohnuki 1995), and the results of platforming for areal leveling on fixed plots (e.g., Fujimoto et al. 1995).

Using results of the tree species segmentation and high-resolution DEM data, several habitat characteristics can be quantified. For instance, habitat altitude of mangrove trees at the Miyara River can be estimated as ranging from − 0.73 to 1.17 m. According to the average tidal range from 2017 to 2021 for Ishigaki port, the mean high water spring (MHWS) is 0.986 m, the mean low water spring is − 0.817 m, and MSL is 0.159 m (JMA). All these values fall within the mangrove habitat zone at the Miyara River. Earlier results of studies suggest that mangrove trees inhabit areas below the high water level of spring tides (FAO 1994), between MSL and the mean high water spring (Pugh 1987; Semeniuk 1994), or between MSL and the mean higher high water (Zhang 2004). In our findings, it was revealed that about 89% of *Bruguiera gymnorrhiza* trees and about 78% of *Rhizophora stylosa* trees were above MSL in the Miyara River mangrove forest. This confirms the suggestion made in previous studies (e.g., Ellison et al. 2022) that the majority of these species inhabit above MSL. This is the study that such elevation frequency by species has been better quantified on a scale of thousands of trees.

In addition, the differences of ranges and peaks of the habitat altitudes of different mangrove species were readily apparent (Fig. 7). The *Rhizophora stylosa* in the lower elevations of the Miyara River mangrove forest mainly grow along the river, whereas those at higher elevations grow in inland areas. This tendency might be affected by the ecological characteristics of the tree species. *Bruguiera gymnorrhiza* is a shade tree that can live in areas with low sunlight exposure (Krauss and Allen 2003). By contrast, *Rhizophora stylosa* prefers places with high sunlight exposure. Moreover, it is strongly tolerant of salt (Smith 1987; Zhang et al. 2021). *Rhizophora stylosa* is also well known as a pioneer tree species in expanding mangrove forests (Kitao et al. 2003). For these differences of characteristics, it is expected that *Rhizophora stylosa* has difficult growing under a *Bruguiera gymnorrhiza* canopy.

4.2 Development process of the mangrove forest

It is also pointed out that changes in the zonation of tree species are linked to the mangrove forest development process (Nakasuga 1979). This study successfully quantified the elevation range of each mangrove tree species, which had been surveyed earlier by transect surveys (Ellison et al. 2022) or quantitative surveys based on the area used by each tree species community using image analysis and ALS point clouds (Zhu et al. 2019).

Comparison of 1978 and 2022 photographs shows that mangrove trees are expanding their habitat in areas not only along the river and creeks but also inland away from the river (Fig. 8). Unlike the orthophotograph, the aerial photograph taken in 1978 includes distortions. In addition, value changes might not be the same between these two photographs because of the differences of the sunlight at the times the aerial photographs were taken and because of the accuracy of the camera. Therefore, quantitative comparison might be difficult, although it is still useful to examine the areas where vegetation has newly increased. Our tree segmentation results revealed *Rhizophora stylosa* as the dominant species in the area where the mangrove habitat area increased during 1978–2022. The expansion of *Rhizophora stylosa*, which has high salt tolerance and which seeks sunlight, toward the river and creeks can imply that a new habitable area for mangrove trees was created because of the gain in elevation with river sediment deposition and sediment trapping

by mangrove trees. This expansion represents a dynamic transition of mangrove forest, as generally considered in earlier studies (Mochida et al. 1999). However, because the distribution of mangrove tree species is strictly controlled by salinity, which is tied to the altitude relative to the tidal range (Marchand et al. 2011), the expansion of *Rhizophora stylosa* landward can be attributed to sea-level rise. Indeed, Okinawa Regional Headquarters, JMA report (2022) stated that the sea-level rise at Ishigaki Port is 2.4 mm per year. Alternatively, there might also be several other possible reasons, such as the ground elevation being lowered to enter the intertidal zone. Further detailed monitoring is required. In any case, it is likely that non-mangrove trees, which are not salt-tolerant, cannot continue to inhabit the area because of the sea-level rise and/or other factors such as the ground lowering. *Rhizophora stylosa*, which is salt-tolerant and which prefers sunlight, could have expanded its habitat to inland areas as a pioneering mangrove tree seeking sunlight.

Based on the findings obtained from this study, future changes of mangrove distributions can be predicted. It can be expected that riverside and inland areas now inhabited by *Rhizophora stylosa* will be surrendered to the spread of *Bruguiera gymnorrhiza*. In addition, *Rhizophora stylosa* might advance its distribution further inland and in riverward directions. However, landward advancement of *Rhizophora stylosa* might soon halt because a steep slope exists at the landward edge of the forest (Fig. 4). Similarly, riverward advancement of *Rhizophora stylosa* might confront some resistance because the area is frequently affected by large typhoons: sediments and trees along the river might constantly be affected by floods.

5 Conclusions

This study was aimed to elucidate the microtopography and spatial distribution of mangrove forests at the Miyara River. This contribution applied LiDAR surveys of two types (ALS and MLS) by focusing on mangrove species and distribution in the mangrove forest. Results revealed that ALS and MLS complement each weakness. Therefore, application of both survey methods is preferable to obtain an overall set of the point clouds of the mangrove forest. By analyzing composite ALS + MLS point clouds, it was also possible to obtain high-precision microtopographic data in a wide area and to understand the spatial distribution of tree species: those were not obtainable using earlier conventional survey methods. The microtopography and spatial distribution of mangrove tree species are fundamental data supporting studies of geomorphology and ecology. Indeed, these data are indispensable for understanding not only the dynamics of the mangrove forest but also for appropriate conservation measures for mangrove forests.

We compared the elevations of tree species using positions of trees with species segmentation and DEM from LiDAR data. The results indicated that *Rhizophora stylosa* has a distribution from an area below the mean tide level and has a wider range of habitat elevations than shown by *Bruguiera gymnorrhiza*. This result and comparison with aerial photographs revealed that *Rhizophora stylosa* has been expanding over 40 years, indicating that, within the restriction of the habitat altitude, the mangrove tree species are changing their habitat area according to the species characteristics under the principle of survival of the fittest. Indeed, *Rhizophora stylosa* has high salt tolerance and prefers sunlight, whereas *Bruguiera gymnorrhiza* has high shade tolerance. Consequently, *Rhizophora stylosa*, which has difficulty growing under *Bruguiera gymnorrhiza*, prefers to expand its habitat areas not only to lower elevations along riverside areas but also to higher elevations inland, seeking sunlight.

Although our dataset has sufficient accuracy to discuss habitat altitudes of mangrove trees, the following should be considered if one wants to obtain a higher accuracy point cloud dataset: (1) Raise the density of ALS point clouds by raising the overlap rates, which makes it easier to infer characteristic points and to combine the MLS point clouds. (2) Do the ALS survey at times when wind speeds are sufficiently low. Wind is regarded as the main factor causing errors in ALS surveys related to device positioning because UAVs are susceptible to wind gusts (Yang et al. 2017). During our ALS survey, the winds were a bit strong (less than 10 m/s), which might have affected measurements. (3) Improve the SLAM accuracy using the MLS survey. By dividing the survey into shorter time periods, error propagation might be reduced. However, it is noteworthy that errors occur when their point clouds are combined.

Abbreviations

LiDAR	Light detection and ranging
SLAM	Simultaneous localization and mapping
UAV	Unmanned aerial vehicle
IMU	Inertial motion unit
ALS	Aerial laser scanning
MLS	Mobile laser scanning
DEM	Digital elevation model
MSL	Mean sea level
MHWS	Mean high water spring
RMSE	Root mean-squared error
MAE	Mean absolute error
VARI	Visible Atmospherically Resistant Index

Acknowledgements

We appreciate H. Takahashi, T. Katono, H. Shibuya, H. Kimura, and K. Nakata for their support during field work and Ishigaki City for approving the survey. Reviewers provided valuable comments on improving our manuscript.

Author contributions
KG proposed the topic and designed the research. All authors conducted field surveys. KK and HY conducted data analyses. KK and KG prepared an original draft. All authors read and approved the final manuscript.

Funding
This research was supported by the Kurita Water and Environment Foundation, the Ministry of Education, Culture, Sports, Science and Technology (MEXT) of Japan, under its Second Earthquake and Volcano Hazards Observation and Research Program (Earthquake and Volcano Hazard Reduction Research) and JSPS KAKENHI Grant Nos. 21H04508 and 21H04379.

Availability of data and materials
The datasets used and/or analyzed during this study are available from the corresponding author on reasonable request.

Declarations

Competing interests
The authors declare no competing interests.

Received: 1 December 2023 Accepted: 7 April 2024
Published online: 15 April 2024

References

Do ANT, Tran HD, Ashley M, Nguyen AT (2022) Monitoring landscape fragmentation and aboveground biomass estimation in Can Gio Mangrove Biosphere Reserve over the past 20 years. Eco Inform 70:101743. https://doi.org/10.1016/j.ecoinf.2022.101743

Donager J, Sánchez Meador A, Blackburn R (2021) Adjudicating perspectives on forest structure: How do airborne, terrestrial, and mobile Lidar-derived estimates compare? Remote Sens 13:2297. https://doi.org/10.3390/rs13122297

Duke N, Ball M, Ellison J (1998) Factors influencing biodiversity and distributional gradients in mangroves. Glob Ecol Biogeogr Lett 7:27–47. https://doi.org/10.2307/2997695

Ellison J, Buffington K, Thorne K, Gesch D, Irwin J, Danielson J (2022) Elevations of mangrove forests of Pohnpei, Micronesia. Estuar Coast Shelf Sci 268:107780. https://doi.org/10.1016/j.ecss.2022.107780

FAO (1994) Mangrove forest management guidelines. Rome: FAO, FAO Forestry Paper 117:5

Fujimoto K, Ohnuki Y (1995) Developmental processes of mangrove habitat related to relative sea-level changes at the mouth of the Urauchi River, Iriomote Island, southwestern Japan. Q J Geogr 47:1–12. https://doi.org/10.5190/tga.47.1

Fujimoto K, Tabuchi R, Mori T, Murohushi T (1995) Site environments and stand structure of the mangrove forests on Pohnpei Island, Micronesia. Jpn Agric Res Q 29:275–284

Gitelson AA, Kaufman YJ, Stark R, Rundquist D (2002) Novel algorithms for remote estimation of vegetation fraction. Remote Sens Environ 80:76–87. https://doi.org/10.1016/S0034-4257(01)00289-9

Hyyppä E, Kukko A, Kaijaluoto R, White JC, Wulder MA, Pyörälä J, Liang X, Yu X, Wang Y, Kaartinen H, Virtanen JP, Hyyppä J (2020) Accurate derivation of stem curve and volume using backpack mobile laser scanning. ISPRS J Photogramm Remote Sens 161:246–262. https://doi.org/10.1016/j.isprsjprs.2020.01.018

Ishikawa T, Okamoto N, Anan R, Ikemi H (2022) Accuracy of the relative positioning with carrier phase observation using low-cost GNSS receivers on campus. Bull Nippon Bunri Univ 50:97–102

Japan Meteorological Agency (undated) Tides for each year. Japanese title was translated by author. https://www.data.jma.go.jp/gmd/kaiyou/db/tide/gaikyo/nenindex.php. Accessed 12 Feb 2024

Kitao M, Utsugi H, Kuramoto S, Tabuchi R, Fujimoto K, Lihpai S (2003) Light-dependent photosynthetic characteristics indicated by chlorophyll fluorescence in five mangrove species native to Pohnpei Island, Micronesia. Physiol Plant 117:376–382. https://doi.org/10.1034/j.1399-3054.2003.00042.x

Knight JM, Dale PE, Spencer J, Griffin L (2009) Exploring LiDAR data for mapping the micro-topography and tidal hydro-dynamics of mangrove systems: an example from southeast Queensland, Australia. Estuar Coast Shelf Sci 85:593–600. https://doi.org/10.1016/j.ecss.2009.10.002

Krauss KW, Allen JA (2003) Factors influencing the regeneration of the mangrove *Bruguiera gymnorrhiza* (L.) Lamk. on a tropical Pacific island. For Ecol Manag 176:49–60. https://doi.org/10.1016/S0378-1127(02)00219-0

Li W, Guo Q, Jakubowski MK, Kelly M (2012) A new method for segmenting individual trees from the Lidar point cloud. Photogramm Eng Remote Sens 78:75–84. https://doi.org/10.14358/PERS.78.1.75

Liu Y, Zhang X, Ma Z, Dong N, Xie D, Li R, Johnston DM, Gao YG, Li Y, Lei Y (2023) Developing a more accurate method for individual plant segmentation of urban tree and shrub communities using LiDAR technology. Landsc Res 48:313–330. https://doi.org/10.1080/01426397.2022.2144813

Macnae W (1969) A general account of the fauna and flora of mangrove swamps and forests in the Indo-West-Pacific region. Adv Mar Biol 6:73–270. https://doi.org/10.1016/S0065-2881(08)60438-1

Marchand C, Allenbach M, Lallier-Vergès E (2011) Relationships between heavy metals distribution and organic matter cycling in mangrove sediments (Conception Bay, New Caledonia). Geoderma 160:444–456. https://doi.org/10.1016/j.geoderma.2010.10.015

Mochida Y, Fujimoto K, Miyagi T, Ishihara S, Murofushi T, Kikuchi T, Pramojanee P (1999) A phytosociological study of the mangrove vegetation in the Malay Peninsula. Tropics 8:207–220

Nakasuga T (1979) Analysis of the mangrove stand. Sci Bull Facul Agric Univ Ryukyus 26:413–519

Nakata K, Yanagisawa H, Goto K (2023) A new point cloud processing method unveiled hidden coastal boulders from deep vegetation. Sci Rep 13:10918. https://doi.org/10.1038/s41598-023-37985-2

Nakaza E, Watanabe Y, Kawahara D, Iribe T, Savou R (2011) Characteristic changes in mangrove forest in Ishigaki Island. J Jpn Soc Civ Eng B3 Mar Dev 67:732–737. https://doi.org/10.2208/JSCEJOE.67.I_732

Niwa H, Ise H, Kamada M (2023) Suitable LiDAR platform for measuring the 3D structure of mangrove forests. Remote Sens 15:1033. https://doi.org/10.3390/rs15041033

Okinawa Regional Headquarters, JMA (2022) Okinawa climate change monitoring report 2022. Japanese title was translated by author. https://www.jma-net.go.jp/okinawa/data/kiko/report/2022_all.pdf. Accessed 12 Feb 2024

Pham TD, Yokoya N, Bui DT, Yoshino K, Friess DA (2019) Remote sensing approaches for monitoring mangrove species, structure, and biomass: opportunities and challenges. Remote Sens 11:230. https://doi.org/10.3390/rs11030230

Pugh DT (1987) *Tides,* surges and mean sea-level: a handbook for engineers and scientists. Wiley, Hoboken, p 396

Saintilan N, Khan NS, Ashe E, Kelleway JJ, Rogers K, Woodroffe CD, Horton BP (2020) Thresholds of mangrove survival under rapid sea level rise. Science 368:1118–1121. https://doi.org/10.1126/science.aba2656

Semeniuk V (1994) Predicting the effect of sea-level rise on mangroves in northwestern Australia. J Coast Res 10:1050–1076

Shao J, Zhang W, Mellado N, Wang N, Jin S, Cai S, Luo L, Lejemble T, Yan G (2020) SLAM-aided forest plot mapping combining terrestrial and mobile laser scanning. ISPRS J Photogramm Remote Sens 163:214–230. https://doi.org/10.1016/j.isprsjprs.2020.03.008

Smith TJ III (1987) Seed predation in relation to tree dominance and distribution in mangrove forests. Ecology 68:266–273. https://doi.org/10.2307/1939257

Tong SS, Pham-Duc B, Phan TH, Pham TL, Tong THA (2023) Investigation of estuarine mangrove ecosystem changes using unmanned aerial vehicle images: case study in Xuan Thuy National Park (Vietnam). Reg Stud Marine Sci 62:102910. https://doi.org/10.1016/j.rsma.2023.102910

Woodroffe CD, Rogers K, McKee KL, Lovelock CE, Mendelssohn IA, Saintilan N (2016) Mangrove sedimentation and response to relative sea-level rise. Ann Rev Mar Sci 8:243–266. https://doi.org/10.1146/annurev-marine-122414-034025

Xie Y, Yang T, Wang T, Chen X, Pang S, Hu J, Wang A, Chen L, Shen Z (2022) Applying a portable backpack Lidar to measure and locate trees in a nature forest plot: accuracy and error analyses. Remote Sens 14:1806. https://doi.org/10.3390/rs14081806

Yamada K, Maegawa S, Toyohara H (2013) Benthic animal contribution to cellulose breakdown in sediments of mangrove estuaries in the southwestern islands of Japan. Plankon Benthos Res 8:96–101. https://doi.org/10.3800/pbr.8.96

Yamamoto A, Miyagi T, Baba S, Furukawa K, Unome S (2023) Preliminary study of understanding the structure of mangrove forests by LiDAR-SLAM. Mangrove Sci 14:3–8

Yang G, Liu J, Zhao C, Li Z, Huang Y, Yu H, Xu B, Yang X, Zhu D, Zhang X, Zhang R, Feng H, Zhao X, Li Z, Li H, Yang H (2017) Unmanned aerial vehicle remote sensing for field-based crop phenotyping: current status and perspectives. Front Plant Sci 8:1111. https://doi.org/10.3389/fpls.2017.01111

Yang Y, Liang X, Wang B, Xie Z, Shen X, Sun X, Zhu X (2022) Biophysical parameters retrieval of mangrove ecosystem using 3D point cloud descriptions from UAV photographs. Eco Inform 72:101845. https://doi.org/10.1016/j.ecoinf.2022.101845

Yin D, Wang L (2019) Individual mangrove tree measurement using UAV-based LiDAR data: possibilities and challenges. Remote Sens Environ 223:34–49. https://doi.org/10.1016/j.rse.2018.12.034

You H, Liu Y, Lei P, Qin Z, You Q (2023) Segmentation of individual mangrove trees using UAV-based LiDAR data. Eco Inform 77:102200. https://doi.org/10.1016/j.ecoinf.2023.102200

Zhang Q (2004) Coastal bio-geomorphologic zonation of coral reefs and mangroves and tide level control. J Coast Res 43:202–211

Zhang W, Qi J, Wan P, Wang H, Xie D, Wang X, Yan G (2016) An easy-to-use airborne LiDAR data filtering method based on cloth simulation. Remote Sens 8:501. https://doi.org/10.3390/rs8060501

Zhang Y, Xin K, Sheng N, Xie Z, Liao B (2021) The regenerative capacity of eight mangrove species based on propagule traits in Dongzhai Harbor, Hainan Province. China Glob Ecol Conserv 30:e01788. https://doi.org/10.1016/j.gecco.2021.e01788

Zhao X, Guo Q, Su Y, Xue B (2016) Improved progressive TIN densification filtering algorithm for airborne LiDAR data in forested areas. ISPRS J Photogramm Remote Sens 117:79–91. https://doi.org/10.1016/j.isprsjprs.2016.03.016

Zhu X, Hou Y, Weng Q, Chen L (2019) Integrating UAV optical imagery and LiDAR data for assessing the spatial relationship between mangrove and inundation across a subtropical estuarine wetland. ISPRS J Photogramm Remote Sens 149:146–156. https://doi.org/10.1016/j.isprsjprs.2019.01.021

Publisher's Note